VEGETATIVE VIGOR OF MAIZE CROP OBTAINED THROUGH VEGETATION INDEXES IN ORBITAL AND AERIAL SENSORS IMAGES

L.S. Santana[1*], G.A e S. Ferraz[1], L.M. Santos[1], D.A. Maciel[2], R.A.P. Barata[1], É. F. Reynaldo[3] and G. Rossi[4]

[1] *UFLA - Federal University of Lavras, Department of Agricultural Engineering, Lavras - MG, Brazil*
[2] *INPE - National Institute of Space Research, Division of Remote Sensing, São José dos Campos – SP, Brazil*
[3] *Maintenance Manager at Syngenta - Uberlândia - MG – Brazil*
[4]*University of Florence, Department of Agriculture, Food, Environment and Forestry (DAGRI), Florence, Italy*

Article history: Received 01 July 2019; Received in revised form 20 July 2019; Accepted 26 July 2019; Available online 30 September 2019.

ABSTRACT

Currently, images from unmanned aerial vehicles (UAVs) are being used due to their high spatial and temporal resolution. Studies comparing different mobile data acquisition platforms, such as satellites, are important due to the limited spatial and temporal resolution of some satellites as well of the presence of clouds in such images. The objective of this study was to compare the vegetation indices (VIs) generated from images obtained by orbital (satellite) and sub-orbital (unmanned aerial vehicles - UAV) platforms. The experiment was conducted in a maize-growing area in Paraná, Brazil. Landsat 8 and UAV images of the study area were collected. Four VIs were applied: NDVI, VIgreen, ExG and VEG. The NDVI was selected as the control and compared with the other VIs. There was a good correlation (0.79) between the NDVI and the VEG for the UAV images. For the Landsat images, the highest correlation found was between the NDVI and the VIgreen derived from UAV images, which was 0.89. It is concluded that the images obtained by UAVs generated better indices, mainly in the dry season.

Keywords: remote sensing, vegetative vigor, precision agriculture, Unmanned Aircraft System (UAS).

VIGOR VEGETATIVO DE CULTURA DE MILHO OBTIDO POR MEIO DE ÍNDICES DE VEGETAÇÃO EM IMAGENS DE SENSORES ORBITAL E AÉREO

RESUMO

Atualmente, imagens de veículos aéreos não tripulados (VANTs) estão sendo utilizadas devido à sua alta †resolução espacial e temporal. Estudos comparando diferentes plataformas de aquisição de dados móveis, como os satélites, são importantes devido à limitada resolução espacial e temporal de alguns satélites, bem como da presença de nuvens em tais imagens. O objetivo deste estudo foi comparar os índices de vegetação (IVs) gerados a partir de imagens obtidas por plataformas orbitais (satélite) e suborbitais (VANT). O experimento foi conduzido em uma área de cultivo de milho no Paraná, Brasil. Imagens Landsat 8 e VANT da área de

* lucas.santana1@estudante.ufla.br

estudo foram coletadas. Quatro IVs foram aplicados: NDVI, VIgreen, ExG e VEG. O NDVI foi selecionado como controle e comparado com os outros IVs. Houve uma boa correlação (0,79) entre o NDVI e o VEG para as imagens do VANT. Para as imagens Landsat, a maior correlação encontrada foi entre o NDVI e o VIgreen derivado de imagens VANT, que foi de 0,89. Conclui-se que as imagens obtidas pelos VANTs geraram melhores índices, principalmente na estação seca.

Palavras-chave: Sensoriamento Remoto, vigor vegetativo, agricultura de precisão, Sistemas de Aeronaves não tripuladas.

INTRODUCTION

Applications of products obtained by remote sensing increasingly include monitoring agriculture and its processes. Remote sensing tools provide time-series data and orbital images with high temporal and spectral resolution. The identification of vegetation levels by means of reflectance in data from the Landsat satellite series can be exploited in several agricultural applications (GRAESSER & RAMANKUTTY, 2017). With a spatial resolution of 30 m, Landsat satellites are able to identify cyclic vegetation phenomena with a vast image collection that extends through 40 years (HE et al., 2015).

One of the difficulties of satellite remote sensing is the revisit time, which on average is 16 days. This makes agricultural applications, specifically those related to water, nutrient and short-cycle crop management, difficult (XUE & SU, 2017). In addition, passive sensors cannot penetrate clouds; therefore, no data are collected on overcast days, making it difficult to collect data during the rainy season.

Given these difficulties, new forms of monitoring have been developed to fill the gaps left by orbital sensors in agricultural monitoring. Currently, some sensors are used aboard remotely piloted aircraft (RPA). Trujillano et al. (2018) note that although satellite images have been widely used for remote sensing applications, their acquisition depends on weather conditions and that the spatial resolution of the images is not good enough to extract features from the crop shape. Image acquisition using unmanned aerial vehicles (UAVs) has become affordable and can be used in a variety of scenarios; it makes it possible reach large areas of land. According to Hassan et al. (2018), the platforms installed in UAVs are not only fast data acquisition systems but also a tool for reducing the costs and labour problems associated with bad weather.

UAVs have broad applicability in agricultural management and provide data different from those obtained by satellites. However, they still have difficulties to surmount, such as high cost, flight height, limited flight autonomy and low spectral capacity. In contrast, this tool offers a high spatial resolution that is independent of the temporal resolution.

Data obtained from UAVs provide reliable and practical information to producers. The exploitation of this tool represents an advance in agriculture by making farmers independent of data provided from external sources (ZHANG & KOVACS, 2012). The future of agricultural data collection is linked to improvements in aerial data collection systems and algorithms applied to raw data (ADÃO et al., 2017). Characterizing the state and growth of crops through remote sensing is important because it supports decision-making in field management (JIN et al., 2018).

RPAs have been systematically explored because their data collection can be specific and, in some functions, does not depend on the absence of clouds and allows the spatial resolution to be

calculated in advance. With pre-defined missions, their flights can generate important data for decision-making in the field with speed and accuracy.

To improve the generated data and make them more reliable, vegetation indices (VIs) are important tools in factors such as the leaf water deficit, level of vigour and vegetative stage. Sayago et al. (2017) found relationships between the surface temperature and VIs in soybeans using sensors from Landsat satellites. Madugundu et al. (2017) evaluated the ability of Landsat and its derived VIs to estimate gross primary productivity in irrigated maize cultivation. According to Jackson et al. (2004), methods based on the normalized difference vegetation index (NDVI) and the normalized difference water index (NDWI) extracted from Landsat sensors are considered sufficient for monitoring plant water content. The first index is currently considered one of the most explored indices.

Data obtained by orbital sensors provide information that can be used in detailed studies of agricultural crops based on raw data and interactions between bands. We highlight the NDVI, which is most commonly used to evaluate vegetation conditions (DING et al., 2014). Duan et al. (2017) concluded that UAV surveys ensure that high-quality NDVI data are generated. Given the various options for agricultural monitoring and the large number of VIs, it is necessary to study the relationships among VIs, seasons and data collection platforms to identify similarities between indices so that professionals can generate reliable products based on RGB and infrared sensors and satisfy their maize cultivation-related research needs. The objective of this study was to analyse data provided by UAVs and from Landsat satellites sensors based on the NDVI, the green vegetation index (VIgreen), the excess green (ExG) and the vegetative index (VEG).

MATERIALS AND METHODS

Study site

The study was conducted in two maize cultivation areas in the state of Paraná (PR), Brazil (Figure 1). Area 1 is in the Candói municipality at geographic coordinates 25°36’47.41” S and 52°2’54.19” W. Area 2 is in the Guarapuava municipality at 25°31'22.44"S and 51°30'16.38" W. According to the Köppen classification with modifications by Alvares et al. (2013), this region is classified as Cfb, a temperate oceanic climate with mild summers. The rainfall is evenly distributed without a dry season, and the mean temperature of the warmer months does not exceed 22 ºC. The amount of precipitation ranges from 1,100 to 2,000 mm. There are severe and frequent frosts with a mean occurrence period of 10 to 25 days annually. The mean temperature in Guarapuava is 16.7 °C. The mean annual rainfall is 1711 mm.

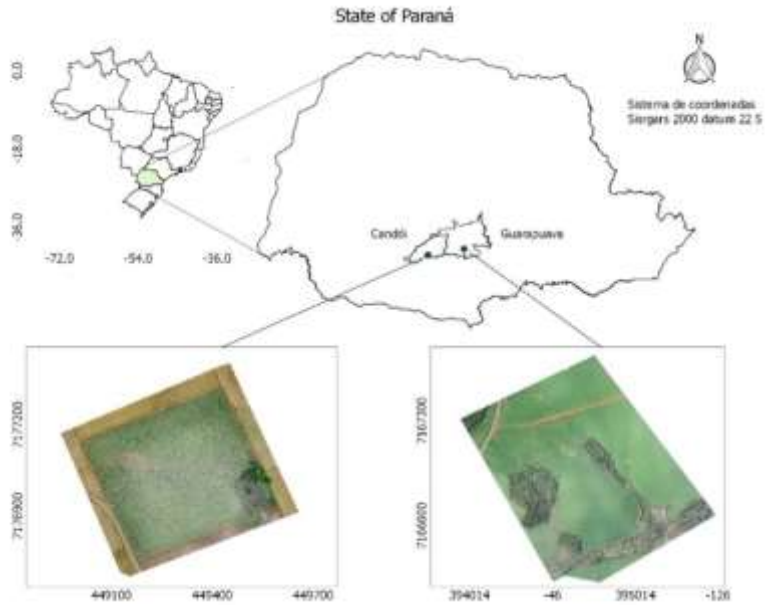

Figure 1. Locations of the study areas: (A) the area near Candói and (B) the area near Guarapuava-PR, Brazil.

The areas under study include the sites of agricultural cultivation with the highest maize production percentages, which is mainly influenced by the predominantly fertile soil. Area 1 (A) contains soil classified as dystrophic dark latosol (EMBRAPA, 2018) during the dry-season harvest. The following mean climatic conditions are observed from February through May: 93 mm of precipitation, temperature of 20.4 °C and relative humidity of 55%. In Area 2 (B), the soils were classified by Embrapa (2018) as humic acric dark latosol (Latossolo Bruno ácrico húmico - LBw) (Guarapuava toposequence) and humic dystrophic red latosol (Latossolo Vermelho distroférrico húmico - LVdf) (Cascavel toposequence).

As shown in Figure 2, the following procedures were performed to complete the proposed objectives.

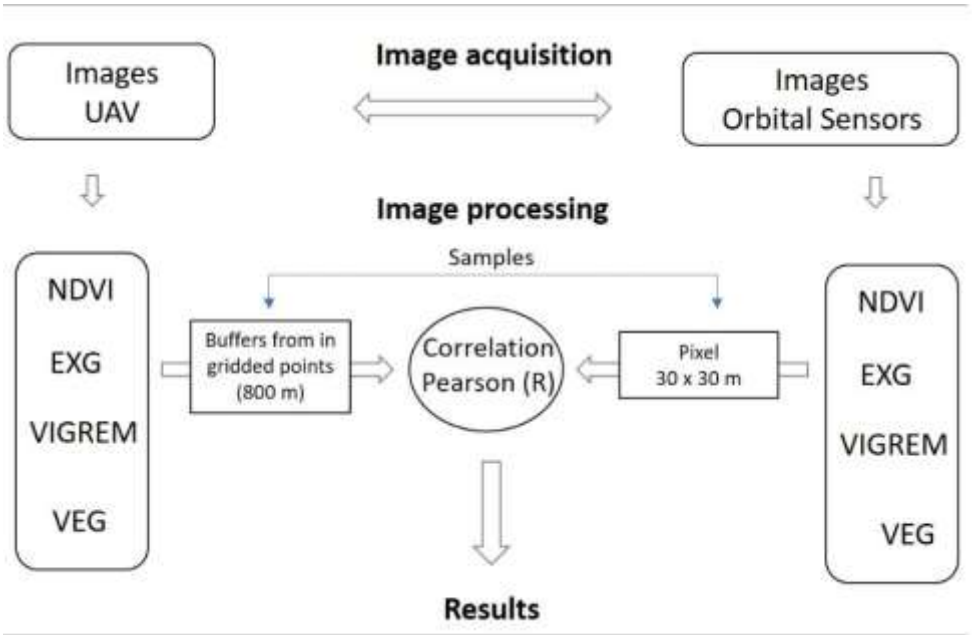

Figure 2 - Flowchart of methodological procedure.

Image acquisition

The images were acquired on 23/09/2015 (area B) and 11/11/2015 (area A) by a UAV with a fixed-wing platform capable of up to 60 minutes of autonomous flight in an autonomous flight controlled by a global navigation satellite system (GNSS) antenna, a pre-defined mission, and a gimbal for stabilizing the camera while the photographs were taken. The UAV used had a coupled digital camera with 20-megapixel resolution in true colour (red-R, green-G and blue-B) with an f/12" aperture and a maximum image size of 4000 × 3000 pixels. With the objective of collecting data of near infrared, it was necessary to block the passage of infra-red. By switching the RGB lens (red, green and blue) by an NGB (near infrared, green and blue) lens.

The satellite images analysed were extracted from the Landsat 8 satellite sensors while it was contemplating the same area as the UAV. The images from 18/01/2016 and 07/04/2016 were acquired from the Earth Explorer site (NASA), LC08_L1TP_orbit-point (222-078),

To correct the effects of the atmosphere Dark Object was applied Subtraction (DOS). Segundo Mather (1999) the atmospheric correction is indispensable for the calculation of vegetation indices, from two or more spectral bands. Because the images are affected differently by the atmospheric scattering.

with the reflectance already corrected for atmospheric effects. These images have eight multispectral bands, including three bands in the visible (RGB) and one band in the NIR, with a spatial resolution of 30 m and a 16-bit radiometric resolution. From the four bands (RGB and NIR), the NDVI, VIgreen, ExG and VEG were calculated.

Image processing

The captured images were stored on an SD card. They were first processed using Agisoft PhotoScan 1.4 (AGISOFT, 2019) to accomplish the following tasks: alignment, construction of the point cloud, densification of the point cloud and generation of the orthomosaic. The images were then exported in GeoTiff format, and later, QuantumGis 2.16.3 (QGIS, 2019) software was used to calculate and analyse the VIgreen, VEG, ExG and NDVI (Table 1).

Table 1. Vegetation Indices used in the study

IV	Name	Equation	Reference
VIgreen	Index Green	$\frac{(G-R)}{(G+R)}$	Gitelson et al. (2002)
VEG	Vegetativen	$VEG = \frac{G}{R^a B^{1-a}}$	Marchant & Onyango (2000)
ExG	Excess of green	$ExG = 2G - R - B$	Woebbecke et al. (1995)
NDVI	Normalized Difference Vegetation Index	$NDVI = \frac{(NIR - R)}{(NIR + R)}$	Rouse et al. (1973)

Where: R - Reflectance obtained from the spectrum in the red region, decimal; G - Reflectance obtained from the spectrum in the green region, decimal; B - Reflectance obtained from the spectrum in the blue region, decimal; NIR - Reflectance of the spectrum in the near infrared region, decimal; A - Constant equal to 0.677.

The satellite images were processed using QGIS 2.16. First, the Landsat 8 L1T images were radiometrically and geometrically corrected. The L1T images were presented by digital number (DN) and were resized to the top-of-atmosphere (TOA) spectral radiance/reflectance. The Landsat 8 images (MS bands and PAN band) were converted to TOA reflectances

using radiometric calibration. Raster calculators were used to generate the VIs for the RGB and NIR spectral bands. To compare the VIs calculated for the satellite and UAV images, the Pearson coefficient was used to compare the NDVI with each calculated VI.

To extract the values from the UAV images, buffers from in gridded points measuring 800 m in diameter were created. This procedure was performed to analyse sufficient numbers of VIs because Landsat 8 satellite images cover areas of 30 m × 30 m, but photogrammetric images only cover areas of 0.03 m × 0.03 m. Figure 3 shows the buffer grid that was created for the UAV images.

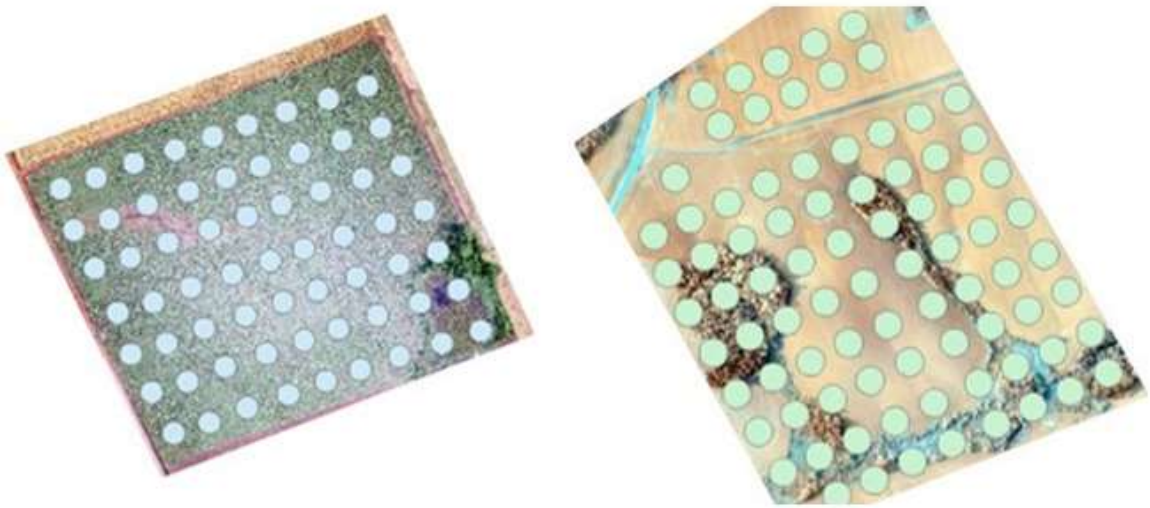

Figure 3. Buffers for extracting data from the UAV images.

After the perimeter of each study area was extracted, the VIs were calculated and subjected to the Pearson correlation test, which is described in equation 5.

$$R_{XY} = \sum_{i=1}^{n} \frac{X_i - \bar{X}}{\sqrt{\sum_{k=1}^{n}(X_k - \bar{X})^2}} \cdot \frac{Y_i - \bar{Y}}{\sqrt{\sum_{k=1}^{n}(Y_k - \bar{Y})^2}} \qquad eq\ (5)$$

This coefficient correlates the two variables X and Y and is formally defined as the covariance of the two variables divided by the standard deviation (which acts as a normalization factor) (DI LENA & MARGARA, 2010).

RESULTS AND DISCUSSION

The image processing and the subsequent calculation of the Pearson R correlation coefficients resulted in the values presented in Table 2, which shows the correlations between the NDVI and the VIgreen, the ExG and the VEG obtained by from the Landsat 8 satellite images. All the vegetation indices and image proportions impact the accuracy of crop classification. It was found that not all vegetation indices have positive impacts, but all can be related to some feature of the study area.

According to Mu et al. (2018), R values equal or close to 1 in a fully supported bivariate distribution express a higher correlation between the data being evaluated, that is, they represent greater significance. Moreover et al. (2005) further subdivided the correlations as follows: R between 0.10 and 0.30 indicates weak correlation; R between 0.40 and 0.6

indicates moderate correlation; R between 0.70 and 1 indicates strong correlation.

Table 2. Results of the Pearson correlation between the NDVI and the VIgreen, ExG and VEG derived from Landsat 8 satellite images of the study areas.

Data	NDVI x Vigreen	NDVI x Exgreen	NDVI x VEG
18/01/2016	0.89	0.70	0.82
07/04/2016	0.54	0.69	0.56

The correlations between the indices from the Landsat 8 remote sensor (Table 2) are significant because most are close to 1 and all represent moderate to strong correlation. However, the comparisons for 18/01/2016 yielded the best results. As shown in Figure 4, the VIgreen presented the strongest correlation with the NDVI. This finding may be related to duplication of the green band, with higher values in areas with more water, because the NDVI responds in the same way.In the "Results and discussion" section all pertinent results should be presented in a logical order and discussed. Discussion portion could also include significance of the results in context of the research field, and suggestions for the future research.

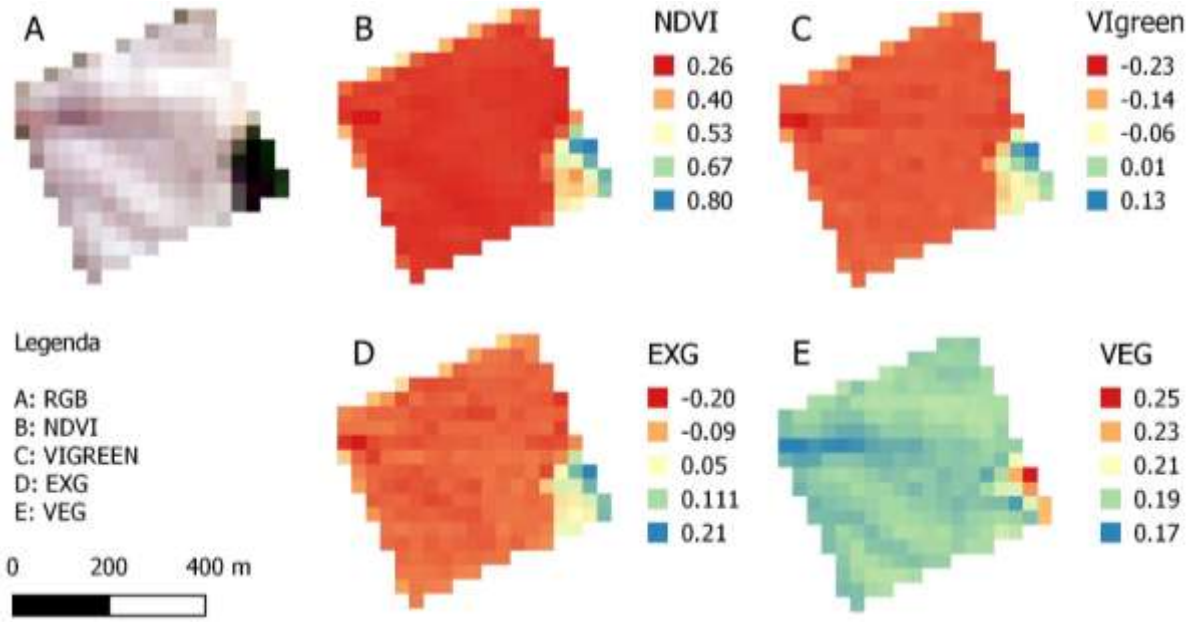

Figure 4. Vegetation indices based on the Landsat 8 image (18/01/2016).

This finding was also observed by Jarlan et al. (2008), who found that when there is more crop vegetation, the indices produce better results because their responses are based on the amount of water present in the leaf. Santos et al. (2015) obtained VIs from Landsat images and found that during the wet season, the values are higher for fully developed crops than they are in the dry season, even with an irrigation system. Neres et al. (2016) showed that the NDVI is low during the dry season and note that this index is limited in its ability to identify areas that have been burned, where it produces low accuracy and numerous false positives. In contrast, in areas with clear water, the NDVI has less spatial variability.

Ke et al. (2015) defended the use of Landsat sensors in times of higher humidity because the signal-to-noise ratio and radiometric sensitivity mean that the Landsat 8 OLI has greater potential for monitoring land surface processes, such as soil cover mapping and change detection,

vegetation growth and evapotranspiration analysis.

Among the values on this date, we highlight the correlation between the NDVI and VIgreen, which reached 0.8897, a value close to 1. Zhang et al. (2016) found a correlation of 0.81 between the VIgreen and the NDVI in two distinct regions, Northeast China and eastern Canada. In that study, indexes were compared and related using the random forest supervised classification algorithm.

For the second date (07/04/2016, Figure 5), the correlations were moderate. This finding is explained by the fact that the crop was in its final vegetative stage, which made it difficult to generate good indices. Despite this, the good response of VEG is highlighted; this did not occur on the first date. This finding shows that this index responds better during the vegetative stage when the moisture content is lower and can be explored with more accuracy in harvest estimates.

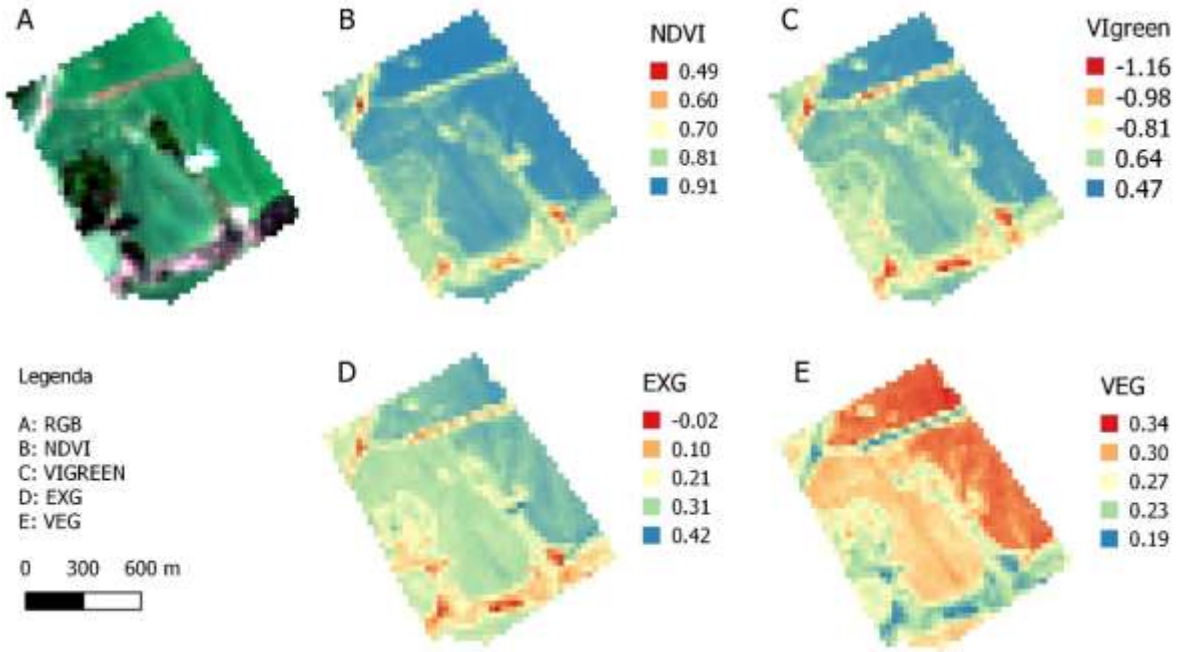

Figure 5. Vegetation indices applied to the Landsat 8 image (07/04/2016).

The values of R for the abovementioned indices obtained from UAV images were also calculated and are presented in Table 3.

Table 3. Pearson correlation (R^2) between the NDVI and the VIgreen, ExG and VEG obtained from UAV images of the study site.

	NDVI x Vigreen	**NDVI x Exgreen**	**NDVI x VEG**
Area 1	0.5078662	0.6185952	0.7883101
Area 2	0.8351776	0.713031	0.8318866

The results obtained from the UAV images (Table 3) show that in Area 1, there was a stronger correlation between the NDVI and VEG at 0.7883. This finding corroborates the study of Torres-Sánchez et al. (2014), who compared the VEG and the ExG obtained from UAV images flying at a height of 60 m and found that the VEG performed better when applied to a wheat crop in Cordoba, Spain. Figure 6 shows the visual similarity between the NDVI and the natural colours; this attests to the high capacity of the index in areas of vigorous vegetation. The similarity between the VEG and the NDVI is also observed.

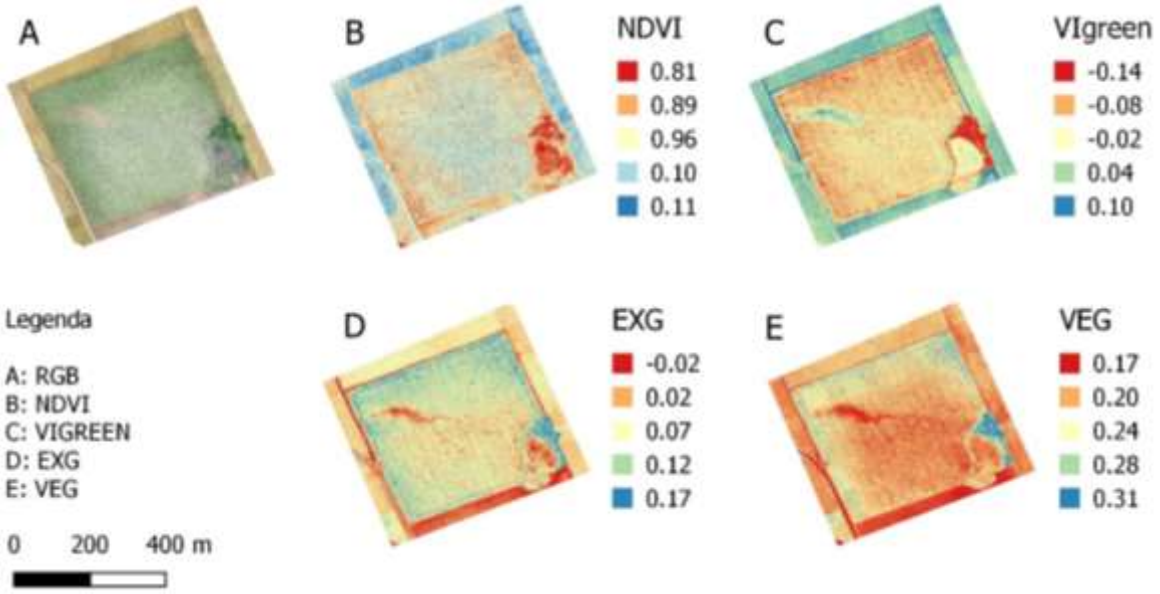

Figure 6. Area A with spectral bands calculated for the vegetation indices.

As shown in Table 3, higher overall correlations were found for Area 2, which was also analysed using the indices found in UAV images. Therefore, better indices were obtained in times of more vigorous vegetation, which is consistent with the Landsat data. This finding may be associated with higher contrast in the reflectance for different bands at this time and to the UAV's ability to decrease natural influences due to its high spatial resolution (Figure 7). The results of Shi et al. (2016) attest to the high monitoring power of UAVs when VIs area calculated based on images of maize and sorghum crops, with more hits occurring in times with more vigorous vegetation. According Juliane et al. (2015), to accurately monitor short-cycle crops with indices in the absence of NIR sensors, it is necessary for the crop to be in a highly vegetative stage. It is stressed that there is a high probability of error in indices that do not include the NIR spectral region.

Another factor to be highlighted is that the absence of a multispectral camera coupled to the UAV may have affected the NIR values, which, in this study, were obtained with the help of a red-band reflectance-blocking filter. This may have led to the low values in Area 1, which was considered the more vegetated area.

So, understanding results from indices that use red locking becomes important. multispectral cameras, equipped with sensors that have the ability to acquire image of the near infrared band, have a high acquisition cost (SILVA, 2016).

Application of modified cameras in agriculture can be defined by the objective of the evaluation. Therefore, it is necessary to decide if a simple unmodified RGB camera or a relatively complex dual-camera system with the NIR band should be selected. Many remote sensing imaging systems based on unmodified single cameras have been used for some agricultural applications to achieve satisfying results (ZHANG et al., 2016).

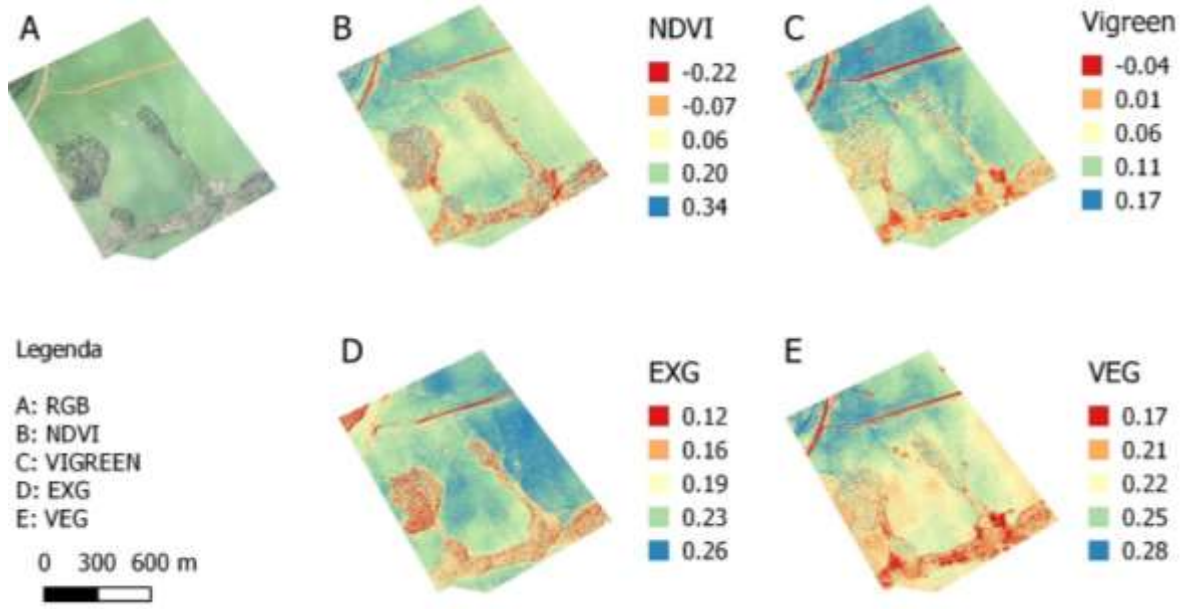

Figure 7. Area B in the vegetation index calculations.

When comparing the correlation coefficients of the different indices obtained from Landsat 8 images to those obtained from UAV images, it was found that both resulted in significant values. However, during the dry season, it is difficult to generate VIs by means of sensors in satellite platforms because the mean infrared band is influenced by water. In contrast, the UAV images resulted in lower correlation coefficients in the more vegetated area than the Landsat 8 images did, which can be attributed to the absence of a multispectral sensor, which may have affected the values for the NIR band, even with the red-blocking filter.

The data provided by the satellite sensors can be used for a wider range of indices because they include 8 spectral bands; however, these data have a spatial resolution of 30 m × 30 m, which may compromise surveys of small areas. Another important point is that the temporal resolution of 16 days can impair monitoring, as in the case of maize, which is considered a seasonal crop, i.e., three to four months pass between planting and harvest.

CONCLUSIONS

According to the comparison between indices based on satellite images and UAV scenes, we note that there are still difficulties with generating vegetation indices. The limitation of UAVs with respect to NIR sensors is apparent; therefore, the practicality of using UAVs and rapid data generation are highlighted. When comparing the seasons, the survey that used UAVs yielded better results.

Regarding the performance of the VIs, the VEG presented the strongest correlation with the NDVI. It is important to note that the VEG is based on the RGB bands, and therefore, the equipment costs less. Satellite sensors have limitations in relation to the stations surveyed, because they are influenced by climatic conditions, low spatial resolutions and high temporal resolutions. Despite this, they were better at generating VIs that use the infrared band when compared to UAVs.

REFERENCES

ADÃO, T.; HRUŠKA, J.; PÁDUA, L.; BESSA, J.; PERES, E.; MORAIS, R.; SOUSA, J. Hyperspectral imaging: A review on UAV-based sensors, data processing and applications for agriculture and forestry. **Remote Sensing**, v. 9(11): 11-10, 2007.

AGISOFT. Software Agisoft PhotoScan. available in: http://www.agisoft.ru/products/photoscan/professional/buy/educational/. Access in: April, 2019.

DI LENA, P.; MARGARA, L. Optimal global alignment of signals by maximization of Pearson correlation. **Information Processing Letters**, v. 110, n. 16: 679-686, 2010.

DING, Y.; ZHAO, K.; ZHENG, X.; JIANG, T. Temporal dynamics of spatial heterogeneity over cropland quantified by time-series NDVI, near infrared and red reflectance of Landsat 8 OLI imagery. **International Journal of Applied Earth Observation and Geoinformation**, v. 30, n. 1: 139–145, 2014.

DUAN, T.; CHAPMAN, S. C.; GUO, Y.; ZHENG, B. Dynamic monitoring of NDVI in wheat agronomy and breeding trials using an unmanned aerial vehicle. **Field Crops Research**, v. 210: 71–80, 2017.

EMBRAPA – Empresa Brasileira de Pesquisas Agropecuária, Sistema Brasileiro de Classificação dos Solos, 590p. 5. ed. 2018.

GITELSON, A. A.; KAUFMAN, Y. J.; STARK, R.; RUNDQUIST, D. Novel algorithms for remote estimation of vegetation fraction. **Remote Sensing of Environment**, v. 80, n. 1: 76–87, 2002.

GRAESSER, J.; RAMANKUTTY, N. Detection of cropland field parcels from Landsat imagery. **Remote Sensing of Environment**, v. 201: 165–180, 2017.

HE, Z.; DU, J.; ZHAO, W.; YANG, J.; CHEN, L.; ZHU, X.; CHANG, X.; LIU, H. Assessing temperature sensitivity of subalpine shrub phenology in semi-arid mountain regions of China. **Agricultural and Forest Meteorology**, v. 213: 42–52, 2015.

JACKSON, T. J.; CHEN, D.; COSH, M.; LI, F.; ANDERSON, M.; WALTHALL, C.; DORIASWAMY, P.; HUNT, E. R. Vegetation water content mapping using Landsat data derived normalized difference water index for corn and soybeans. **Remote Sensing of Environment**, v. 92, n. 4: 475–482, 2004.

JARLAN, L.; MANGIAROTTI, S.; MOUGIN, E.; MAZZEGA, P.; HIERNAUX, P.; LE DANTEC, V. Assimilation of SPOT/VEGETATION NDVI data into a sahelian vegetation dynamics model. **Remote Sensing of Environment**, v. 112, n. 4: 1381–1394, 2008.

JIN, X.; KUMAR, L.; LI, Z.; FENG, H.; XU, X.; YANG, G.; WANG, J. A review of data assimilation of remote sensing and crop models. **European Journal of Agronomy**, v. 92: 141–152, 2018.

MADUGUNDU, R.; AL-GAADI, K. A.; TOLA, E.; KAYAD, A. G.; JHA, C. S. Estimation of gross primary production of irrigated maize using Landsat-8 imagery and Eddy Covariance data. **Saudi Journal of Biological Sciences**, v. 24, n. 2: 410–420, 2017.

MATHER P, M. **Computer processing of remotely-sensed images: an introduction**. New York: John Wiley & Sons; 1999. p. 292.

MARCHANT, J. A.; ONYANGO, C. M. Shadow-invariant classification for scenes

illuminated by daylight. **Journal of the Optical Society of America A**, v. 17, n. 11: 1952-1961, 2000.

MU, Y.; LIU, X.; WANG, L. A Pearson's correlation coefficient-based decision tree and its parallel implementation. **Information Sciences**, v. 435: 40–58, 2018.

QGIS DEVELOPMENT TEAM. QGIS Geographic Information System. Open Source Geospatial Foundation Project. URL:http://qgis.osgeo.org. Access in: April, 2019.

SILVA, R. DE S. V. Uso de imagens multiespectrais de baixo custo para classificar níveis de N aplicados ao solo em agricultura de precisão. Dissertação. 56p. 2016.

ROUSE, J. W.; HAAS, R. H.; SCHEEL, J. A.; DEERING, D. W. Monitoring Vegetation Systems in the Great Plains with ERTS. 3rd Earth Resource Technology Satellite (ERTS) Symposium. In **Proc. Conf**: 309-317, 1973.

SAYAGO, S.; OVANDO, G.; BOCCO, M. Landsat images and crop model for evaluating water stress of rainfed soybean. **Remote Sensing of Environment**, v. 198: 30–39, 2017.

TORRES-SÁNCHEZ, J.; PEÑA, J. M.; DE CASTRO, A. I.; LÓPEZ-GRANADOS, F. Multi-temporal mapping of the vegetation fraction in early-season wheat fields using images from UAV. **Computers and Electronics in Agriculture**, v. 103: 104–113, 2014.

WOEBBECKE, D. M.; MEYER, G. E.; VON BARGEN, K.; MORTENSEN, D. A. Shape features for identifying young weeds using image analysis. **Transactions of the ASAE (American Society of Agricultural Engineers)**, v. 38, n. 1, p. 271–281, 1995.

ZHANG, C.; KOVACS, J. M. The application of small unmanned aerial systems for precision agriculture: A review. **Precision Agriculture**, v. 13, n. 6: 693–712, 2012.

ZHANG, J.; YANG C.; SONG, H.; HOFFMANN, W.; ZHANG, D.; ZHANG, G. Evaluation of an airborne remote sensing platform consisting of two consumer-grade cameras for crop identification. **Remote Sensing**, v. 8, n. 3, p. 257, 2016.